Energy-Band Structure of Germanium and Silicon: The k·p Method*

MANUEL CARDONA AND FRED H. POLLAK
Physics Department, Brown University, Providence, Rhode Island
(Received 13 August 1965)

The energy bands of germanium and silicon, throughout the entire Brillouin zone, have been obtained by diagonalizing a $\mathbf{k}\cdot\mathbf{p}$ Hamiltonian referred to 15 basis states at $\mathbf{k}=0$. The basis states of the $\mathbf{k}\cdot\mathbf{p}$ Hamiltonian correspond to plane-wave states of wave vector (in units of $2\pi/a$) [000], [111], and [200]. For matrix elements and energy gaps we have used, when available, experimental data from cyclotron resonance and optical measurements. The parameters not available from experimental information have been adjusted until the calculated energy bands agree with ultraviolet reflection data. The energies of the Λ_3-Λ_1 transition for germanium and the Σ_4-Σ_1 transition for germanium and silicon, which were not explicitly fitted, are in good agreement with experimental data. The eigenvectors of the $\mathbf{k}\cdot\mathbf{p}$ matrix provide an expansion of the wave function for any value of $\mathbf{k}$ in terms of the $\mathbf{k}=0$ basis states. These eigenvectors have been used (1) to calculate effective masses of the lowest conduction bands in germanium (L_1) and silicon (Δ_1), which are in good agreement with experiment, and (2) to calculate the effects of the spin-orbit interaction on the band structure of germanium. The extension of the $\mathbf{k}\cdot\mathbf{p}$ method to calculate the band structure of zinc-blende- and wurtzite-type materials from that of the isoelectronic group IV material is discussed briefly.

I. INTRODUCTION

THE $\mathbf{k}\cdot\mathbf{p}$ method has been extremely successful in establishing relationships between various band parameters of semiconductors. One of its earliest applications was the derivation of the sum rule for the effective masses.[1] The method was extended to include degenerate bands[2] and the effect of spin-orbit interaction.[3] In this approach expressions for the energy in the vicinity of a high symmetry point of $\mathbf{k}$ space involving a number of parameters are obtained. These parameters are usually determined from experiments such as cyclotron resonance, optical absorption, etc.

The expression obtained for a nondegenerate band as a function of $\Delta\mathbf{k}$ by the use of first- and second-order perturbation theory has been extended to larger values of $\Delta\mathbf{k}$ by the use of degenerate perturbation theory.[4] This type of analysis has been successfully used for interpreting observed nonparabolicities in the band structure of small band-gap semiconductors.

Since the Bloch functions at $\mathbf{k}=0$ form a complete set of periodic functions it is possible to expand the cell periodic part of the wave functions at any value of $\mathbf{k}$ in terms of the Bloch functions at $\mathbf{k}=0$. Therefore, the diagonalization of the $\mathbf{k}\cdot\mathbf{p}$ Hamiltonian referred to the basis states at $\mathbf{k}=0$ should yield the correct energy bands and wave functions across the entire Brillouin zone (B.Z.) if enough basis states are taken. In the past it has been felt that too many states and hence too many parameters are involved for this method to be extended throughout the entire B.Z. We have obtained the correct energy bands across the entire zone for germanium and silicon (neglecting the spin-orbit interaction) by diagonalizing a 15×15 $\mathbf{k}\cdot\mathbf{p}$ Hamiltonian. The 15 states used correspond to free-electron states having wave vector (in units of $2\pi/a$) [000], [111], and [200]. It is possible to determine the parameters of the $\mathbf{k}\cdot\mathbf{p}$ Hamiltonian so as to fit all the available experimental data for these materials. The effects of the spin-orbit interaction are determined by two additional parameters which can be calculated from available experimental data for germanium.

The expansion of the wave functions in terms of wave functions for $\mathbf{k}=0$ makes it possible to calculate a number of parameters of interest, such as matrix elements of the momentum $\mathbf{p}$ and effective masses for any value of $\mathbf{k}$.

By a combination of this method and the pseudopotential technique it is possible to calculate the effect of hydrostatic pressure on the energy bands of these materials.

II. THE k·p HAMILTONIAN

Consider the nonrelativistic one-electron Schrödinger equation (in atomic units):

$$[-\nabla^2+V(\mathbf{r})]\Psi=E\Psi, \qquad (1)$$

where $V(\mathbf{r})$ is a potential having the periodicity of the lattice. The solutions to Eq. (1) are the Bloch functions $\Psi=\exp(i\mathbf{k}\cdot\mathbf{r})\times u_{n,\mathbf{k}}(\mathbf{r})$, where $u_{n,\mathbf{k}}(\mathbf{r})$ has the periodicity of the crystal lattice. By substituting the Bloch functions in Eq. (1) one obtains:

$$[H_0+2\mathbf{k}\cdot\mathbf{p}+k^2]u_{n,\mathbf{k}}(\mathbf{r})=E_n(\mathbf{k})u_{n,\mathbf{k}}(\mathbf{r}), \qquad (2)$$

where H_0 is the Hamiltonian for $\mathbf{k}=0$. The term k^2 of Eq. (2) is a c number and can be considered as a shift in all the eigenvalues $E_n(\mathbf{k})$. The term $2\mathbf{k}\cdot\mathbf{p}$ is the standard $\mathbf{k}\cdot\mathbf{p}$ Hamiltonian. When Eq. (2) is written in matrix form with respect to the states at $\mathbf{k}=0$, H_0 and k^2 have only diagonal elements and the term $\mathbf{k}\cdot\mathbf{p}$ has only nondiagonal terms in a crystal with inversion symmetry. The number of independent $\mathbf{k}\cdot\mathbf{p}$ matrix elements is greatly reduced by group-theoretical selec-

* Supported in part by the Advanced Research Projects Agency and the National Science Foundation.
[1] F. Seitz, *Modern Theory of Solids* (McGraw-Hill Book Company, Inc., New York, 1940), p. 352.
[2] W. Shockley, Phys. Rev. 78, 173 (1950).
[3] G. Dresselhaus, A. F. Kip, and C. Kittel, Phys. Rev. 98, 368 (1955); E. O. Kane, J. Phys. Chem. Solids 1, 82 (1956).
[4] E. O. Kane, J. Phys. Chem. Solids 4, 249 (1957).

TABLE I. Eigenvalues (in rydbergs) of the states used in the $\mathbf{k}\cdot\mathbf{p}$ Hamiltonian for germanium and silicon together with the eigenvalues of these states as calculated by the O.P.W. and pseudopotential methods. The corresponding plane-wave and atomic states (in parentheses) are also given.

Crystal states at $\mathbf{k}=0$	Corresponding plane-wave and atomic states	Germanium: Eigenvalues used in $\mathbf{k}\cdot\mathbf{p}$ Hamiltonian	Germanium: O.P.W. method[a]	Germanium: Pseudopotential method	Silicon: Eigenvalues used in $\mathbf{k}\cdot\mathbf{p}$ Hamiltonian	Silicon: O.P.W. method[a]	Silicon: Pseudopotential method
$\Gamma_{25'}{}^{l}$	[111] (p^+)	0.00	0.00	0.00	0.00	0.00	0.00
$\Gamma_{2'}{}^{l}$	[111] (s^-)	0.0728[b]	−0.081	−0.007	0.265[b]	0.164	0.23
Γ_{15}	[111] (p^-)	0.232[b]	0.231	0.272	0.252[b]	0.238	0.28
$\Gamma_1{}^{u}$	[111] (s^+)	0.571	0.571	0.444	0.520	0.692	0.52
$\Gamma_1{}^{l}$	[000] (s^+)	−0.966	−0.929	−0.950	−0.950	−0.863	−0.97
$\Gamma_{12'}$	[200] (d^-)	0.770	0.770	0.620	0.710	0.696	0.71
$\Gamma_{25'}{}^{u}$	[200] (d^+)	1.25[c]		0.890	0.940		0.94
$\Gamma_{2'}{}^{u}$	[200] (s^-)	1.35		0.897	0.990		0.99

[a] Reference 9. [b] Reference 8. [c] Reference 3.

tion rules in high-symmetry crystals. In particular, for materials with inversion symmetry, only matrix elements between states of opposite parity are allowed.

For the case of the many-electron Hamiltonian, Kane[5] has shown that in Eq. (2) the $\mathbf{k}\cdot\mathbf{p}$ term must be replaced by $-i[\mathbf{r},H]\cdot\mathbf{k}$ ($\mathbf{r}$ is the position vector and H the many-body Hamiltonian) and k^2 replaced by

$$-\tfrac{1}{2}\sum_{\mu,\nu} k_\mu k_\nu [r_\mu,[r_\nu,H]]. \tag{3}$$

Terms higher than second order in $\mathbf{k}$ also appear in Eq. (2). The term $[\mathbf{r},H]$ has the same symmetry as the linear momentum $\mathbf{p}$ and hence if one regards the matrix elements of $\mathbf{p}$ as adjustable parameters no modification of the $\mathbf{k}\cdot\mathbf{p}$ Hamiltonian is introduced by the replacement of $\mathbf{p}$ by $2i[\mathbf{r},H]$. Equation (3) equals exactly k^2 if the Hartree Hamiltonian is used but not for the Hartree-Fock Hamiltonian. However, the difference has been estimated to be small.

When the spin-orbit Hamiltonian $(\alpha/2)^2[\nabla V\times\mathbf{p}]\cdot\boldsymbol{\sigma}$ (where $\alpha^2=1/c^2$ in atomic units) is added to the Hamiltonian of Eq. (1), two new terms are generated in Eq. (2). They correspond to the following addition to the $\mathbf{k}\cdot\mathbf{p}$ Hamiltonian of Eq. (2):

$$(\alpha/2)^2[(\nabla V\times\mathbf{p})\cdot\boldsymbol{\sigma}+(\nabla V\times\mathbf{k})\cdot\boldsymbol{\sigma}]. \tag{4}$$

Since the second term in Eq. (4) is usually much smaller than the first, it will be neglected in these calculations.

The effect of the $\mathbf{k}$-dependent spin-orbit interaction and other relativistic corrections on the $\mathbf{k}\cdot\mathbf{p}$ Hamiltonian has been treated by Pratt and Ferreira.[6] In their treatment the term $2\mathbf{p}$ is replaced by

$$-2i\nabla-(\alpha/2)^2(\nabla V\times\boldsymbol{\sigma})-i\alpha^2\nabla^2\nabla +\alpha^2(\mathbf{k}\cdot\nabla)\nabla+(\alpha^2/2)\nabla^2\mathbf{k}. \tag{5}$$

The second term in Eq. (5) is the $\mathbf{k}$-dependent contribution to the spin-orbit interaction. The third term is automatically included in the nonrelativistic $\mathbf{k}\cdot\mathbf{p}$ method if the matrix elements of $\mathbf{p}$ are treated as adjustable parameters to be determined from experiment. The fourth and fifth terms change the form of the $\mathbf{k}\cdot\mathbf{p}$ Hamiltonian, but an estimate based on free-electron wave functions shows that their contribution to the band energies is smaller than 10^{-4} Ry.

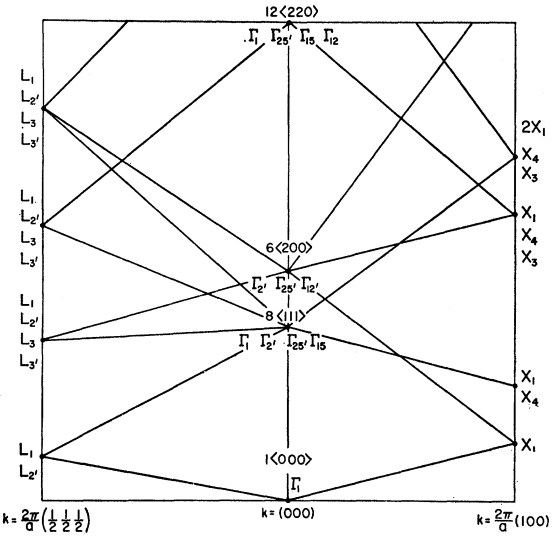

FIG. 1. Energy bands for the "empty" germanium lattice.

[5] E. O. Kane, in *The Properties of the III–V Compounds* (Academic Press Inc., New York, to be published).

[6] G. W. Pratt, Jr. and L. G. Ferreira, in *Proceedings of the International Conference on the Physics of Semiconductors, Paris, 1964* (Dunod Cie., Paris, 1964), p. 69.

TABLE II. Matrix elements of the linear momentum $\mathbf{p}$ (in atomic units) as obtained from the $\mathbf{k}\cdot\mathbf{p}$ method, the pseudopotential method, and cyclotron resonance.

Matrix elements of $\mathbf{p}$	Germanium $\mathbf{k}\cdot\mathbf{p}$ method	Germanium Pseudopotential method	Germanium Cyclotron resonance	Silicon $\mathbf{k}\cdot\mathbf{p}$ method	Silicon Pseudopotential method	Silicon Cyclotron resonance
$P(2i\langle\Gamma_{25'}{}^{l}\vert\mathbf{p}\vert\Gamma_{2'}{}^{l}\rangle)$	1.360	1.24	1.36[a]	1.200	1.27	1.20[b]
$Q(2i\langle\Gamma_{25'}{}^{l}\vert\mathbf{p}\vert\Gamma_{15}\rangle)$	1.070	0.99	1.07[a]	1.050	1.05	1.05[b]
$R(2i\langle\Gamma_{25'}{}^{l}\vert\mathbf{p}\vert\Gamma_{12'}\rangle)$	0.8049	0.75	0.92[c]	0.830	0.74	0.68[d]
$P''(2i\langle\Gamma_{25'}{}^{l}\vert\mathbf{p}\vert\Gamma_{2'}{}^{u}\rangle)$	0.1000	0.09		0.100	0.10	
$P'(2i\langle\Gamma_{25'}{}^{u}\vert\mathbf{p}\vert\Gamma_{2'}{}^{l}\rangle)$	0.1715	0.0092		−0.090	−0.10	
$Q'(2i\langle\Gamma_{25'}{}^{u}\vert\mathbf{p}\vert\Gamma_{15}\rangle)$	−0.752	−0.65		−0.807	−0.64	
$R'(2i\langle\Gamma_{25'}{}^{u}\vert\mathbf{p}\vert\Gamma_{12'}\rangle)$	1.4357	1.13		1.210	1.21	
$P'''(2i\langle\Gamma_{25'}{}^{u}\vert\mathbf{p}\vert\Gamma_{15}\rangle)$	1.6231	1.30		1.320	1.37	
$T(2i\langle\Gamma_{1}{}^{u}\vert\mathbf{p}\vert\Gamma_{15}\rangle)$	1.2003	1.11		1.080	1.18	
$T'(2i\langle\Gamma_{1}{}^{l}\vert\mathbf{p}\vert\Gamma_{15}\rangle)$	0.5323	0.41		0.206	0.34	

[a] Reference 11.
[b] Reference 12.
[c] Calculated from cyclotron-resonance data [T. R. Loree and R. N. Dexter (private communication)] and the value of $\Gamma_{25'}{}^{l}-\Gamma_{12'}$ energy gap used in the $\mathbf{k}\cdot\mathbf{p}$ Hamiltonian of germanium (see Table I).
[d] Calculated from the cyclotron-resonance data of Ref. 12 and the value of $\Gamma_{25'}{}^{l}-\Gamma_{12'}$ energy gap used in the $\mathbf{k}\cdot\mathbf{p}$ Hamiltonian of silicon (see Table I).

III. k·p HAMILTONIAN FOR GERMANIUM AND SILICON

Figure 1 shows the energy bands for the "empty" germanium lattice in the [100] and [111] directions and the symmetries of the various plane-wave states. The real energy bands for a material of this family are obtained by a small perturbation of the empty lattice bands. The large energy gap between the $(2\pi/a)$[200] and the $(2\pi/a)$[220] plane waves of Fig. 1 suggests the possibility of a $\mathbf{k}\cdot\mathbf{p}$ description of the energy bands of germanium and silicon using as a basis only the 15 states of the real crystal which correspond to [000], $(2\pi/a)$[111], and $(2\pi/a)$[200] plane-wave states in the empty lattice. These 15 states and the corresponding plane-wave and atomic states are listed in Table I. The superscripts u and l are used to distinguish between the upper and lower $\Gamma_{2'}$, Γ_1, and $\Gamma_{25'}$ states. The $\Gamma_{25'}{}^{l}$ state is taken to be the origin of energies.

Since the Hamiltonian of Eq. (1) is real, the wave functions at $\mathbf{k}=0$ can be chosen to be real. However, in order to get only real matrix elements of $\mathbf{p}$ and hence a real $\mathbf{k}\cdot\mathbf{p}$ Hamiltonian, the even-parity wave functions have been taken as real and the odd-parity wave functions as pure imaginary. The $\Gamma_{25'}$ wave functions are taken to transform like $X=yz$, $Y=xz$, and $Z=xy$, where x, y, and z are the coordinates with respect to the cubic axes. The Γ_{15} wave functions are taken to transform like x, y, and z. The $\Gamma_{12'}$ wave functions are taken to have the symmetry of $\sqrt{3}(y^2-z^2)(\Gamma_{12'}{}^{(1)})$ and $3x^2-r^2(\Gamma_{12'}{}^{(2)})$.[7] By using the proper selection rules it can be seen that the $\mathbf{k}\cdot\mathbf{p}$ Hamiltonian is determined by 10 matrix elements of $\mathbf{p}$. These are listed in Table II together with the shorthand notation used for them in this paper. Matrix elements of $\mathbf{p}$ between: (1) a $\Gamma_{25'}$ and a $\Gamma_{2'}$ state are labeled P, (2) a $\Gamma_{25'}$ and the Γ_{15} state are called Q, (3) a $\Gamma_{25'}$ and the $\Gamma_{12'}{}^{(1)}$ state are designated by R, and (4) the Γ_{15} and a Γ_1 state are called T. The matrix elements between an X state and $\Gamma_{12'}{}^{(2)}$ are zero.

By means of a suitable rotation of the basis functions the 15×15 $\mathbf{k}\cdot\mathbf{p}$ Hamiltonian can be easily factorized in the [100], [111], and [110] directions.

[100] Direction

In this direction the 3 doubly degenerate Δ_5 bands (which originate at $\Gamma_{25'}{}^{l}$, Γ_{15}, and $\Gamma_{25'}{}^{u}$) are obtained by diagonalizing the 3×3 matrix given below

$$\begin{Vmatrix} k_x^2 & Qk_x & 0 \\ Qk_x & E(\Gamma_{15})+k_x^2 & Q'k_x \\ 0 & Q'k_x & E(\Gamma_{25'}{}^{u})+k_x^2 \end{Vmatrix}. \quad (6)$$

The three Δ_1 bands, which include the lowest conduction band in silicon, are obtained from the 3×3 matrix

$$\begin{Vmatrix} E(\Gamma_{15})+k_x^2 & Tk_x & T'k_x \\ Tk_x & E(\Gamma_1{}^{u})+k_x^2 & 0 \\ T'k_x & 0 & E(\Gamma_1{}^{l})+k_x^2 \end{Vmatrix}. \quad (7)$$

The $\Gamma_{12'}{}^{(2)}$ state does not interact with any other state in the [100] direction and hence produces a band analogous to a free-electron band. The only $\mathbf{k}\cdot\mathbf{p}$ interaction with this band comes from higher lying $\Gamma_{15'}$ states which have been neglected in our 15×15 Hamiltonian. Unless this interaction is included the $\Gamma_{12'}{}^{(2)}$ band will not reach the edge of the B.Z. with zero slope, as required by crystal symmetry. However, since in the vicinity of the X point this band does not seem to be observable in any measurements, no attempt has been made to bring its slope to zero at the zone edge.

[7] The functions γ_1^- and γ_2^- used for $\Gamma_{12'}$ in Ref. 3 are related to $\Gamma_{12'}{}^{(1)}$ and $\Gamma_{12'}{}^{(2)}$ by the relationships $\Gamma_{12'}{}^{(1)}=(1/\sqrt{2})(\gamma_1^--\gamma_2^-)$ and $\Gamma_{12'}{}^{(2)}=(1/\sqrt{2})(\gamma_1^-+\gamma_2^-)$.

The five remaining states can be found by diagonalizing the matrix

$$\begin{Vmatrix} E(\Gamma_{2'}{}^{l})+k_x^2 & Pk_x & 0 & P'k_x & 0 \\ Pk_x & k_x^2 & \sqrt{2}Rk_x & 0 & P''k_x \\ 0 & \sqrt{2}Rk_x & E(\Gamma_{12'})+k_x^2 & \sqrt{2}R'k_x & 0 \\ P'k_x & 0 & \sqrt{2}Rk_x & E(\Gamma_{25'}{}^{u})+k_x^2 & P'''k_x \\ 0 & P''k_x & 0 & P'''k_x & E(\Gamma_{2'}{}^{u})+k_x^2 \end{Vmatrix}. \tag{8}$$

[111] Direction

In the [111] direction also the Hamiltonian can be easily factorized by transforming the Γ_{15} basis functions to functions having the symmetry of $\bar{x}$, $\bar{y}$, and $\bar{z}$, the coordinates referred to a set of axes with $\bar{z}$ along the [111] direction. The $\Gamma_{25'}$ wave functions are transformed to have symmetry $\bar{X}=\bar{y}\bar{z}$, $\bar{Y}=\bar{x}\bar{z}$, and $\bar{Z}=\bar{x}\bar{y}$ while the $\Gamma_{12'}$ functions are chosen to be $\bar{\Gamma}_{12'}{}^{(1)}=\frac{1}{2}[\sqrt{3}\Gamma_{12'}{}^{(1)}-\Gamma_{12'}{}^{(2)}]$ and $\bar{\Gamma}_{12'}{}^{(2)}=\frac{1}{2}[\Gamma_{12'}{}^{(1)}+\sqrt{3}\Gamma_{12'}{}^{(2)}]$.

One finds four doubly degenerate Λ_3 bands given by the Hamiltonian

$$\begin{Vmatrix} k^2 & -(1/\sqrt{3})Qk & 0 & Rk \\ -(1/\sqrt{3})Qk & E(\Gamma_{15})+k^2 & -(1/\sqrt{3})Q'k & 0 \\ 0 & -(1/\sqrt{3})Q'k & E(\Gamma_{25'n})+k^2 & R'k \\ Rk & 0 & R'k & E(\Gamma_{12'})+k^2 \end{Vmatrix}, \tag{9}$$

where $k^2=k_x^2+k_y^2+k_z^2$.

The remaining states, including the lowest conduction band of germanium, are given by the 7×7 matrix

$$\begin{Vmatrix} E(\Gamma_{2'}{}^{l})+k^2 & Pk & 0 & P'k & 0 & 0 & 0 \\ Pk & k^2 & (2/\sqrt{3})Qk & 0 & 0 & 0 & P''k \\ 0 & (2/\sqrt{3})Qk & E(\Gamma_{15})+k^2 & (2/\sqrt{3})Q'k & Tk & T'k & 0 \\ P'k & 0 & (2/\sqrt{3})Q'k & E(\Gamma_{25'}{}^{u})+k^2 & 0 & 0 & P'''k \\ 0 & 0 & Tk & 0 & E(\Gamma_1{}^{u})+k^2 & 0 & 0 \\ 0 & 0 & T'k & 0 & 0 & E(\Gamma_1{}^{l})+k^2 & 0 \\ 0 & P''k & 0 & P'''k & 0 & 0 & E(\Gamma_{2'}{}^{u})+k^2 \end{Vmatrix}. \tag{10}$$

In the [110] direction the 15×15 Hamiltonian can be factorized into a 6×6, a 5×5, a 3×3, and a 1×1 matrix. These matrices will not be written out explicitly in this paper.

IV. CHOICE OF PARAMETERS

In germanium the energies of the $\Gamma_{2'}{}^{l}$ and Γ_{15} state are known from optical measurements.[8] For silicon $E(\Gamma_{15})$ also is known from direct measurements while $E(\Gamma_{2'}{}^{l})$ can be estimated from data for Ge-Si alloys.[8] Although no experimental information is available concerning the remaining eigenvalues at $\mathbf{k}=0$, several of them have been calculated using the orthogonalized-plane-wave (O.P.W.) technique.[9] It is also possible to calculate approximate values for these states by the pseudopotential method if one assumes that only the pseudopotential interaction between our 15 plane-wave states is important. Under this assumption the Γ_{15} and $\Gamma_{12'}$ states have the free-electron energy $[E(\Gamma_{15})=3(2\pi/a)^2$ and $E(\Gamma_{12'})=4(2\pi/a)^2]$. The energies of the remaining states can be obtained by solving 2×2 matrices using the three pseudopotential parameters of Brust for germanium and silicon.[10] This procedure also yields the wave functions at $\mathbf{k}=0$ as a linear combination of [000], [111], and [200] plane waves and therefore it is possible to estimate the matrix elements of $\mathbf{p}$ for the $\mathbf{k}\cdot\mathbf{p}$ Hamiltonian (as will be shown later it is possible to start with any approximate values of the matrix elements of $\mathbf{p}$, for example the free-electron values).

The eigenstates $\Gamma_1{}^{u}$ and $\Gamma_1{}^{l}$ are obtained from the Hamiltonian

$$\begin{Vmatrix} 0 & 2V_p(3) \\ 2V_p(3) & 3(2\pi/a)^2+3V_p(8) \end{Vmatrix}, \tag{11}$$

where the zero of energy is now the bottom of the free-electron bands. Likewise $E(\Gamma_{2'}{}^{l})$ and $E(\Gamma_{2'}{}^{u})$ are obtained from the matrix:

$$\begin{Vmatrix} 3(2\pi/a)^2+3V_p(8) & (6)^{1/2}[V_p(11)+V_p(3)] \\ (6)^{1/2}[V_p(11)+V_p(3)] & 4(2\pi/a)^2+4V_p(8) \end{Vmatrix} \tag{12}$$

and the energies of the two $\Gamma_{25'}$ states are found by solving

$$\begin{Vmatrix} 3(2\pi/a)^2-V_p(8) & \sqrt{2}[V_p(3)-V_p(11)] \\ \sqrt{2}[V_p(3)-V_p(11)] & 4(2\pi/a)^2 \end{Vmatrix}. \tag{13}$$

[8] For a compilation of optical data for germanium, silicon, and zinc-blende-type materials see M. Cardona, J. Phys. Chem. Solids 24, 1543 (1963).

[9] F. Herman, in *Proceedings of the International Conference on the Physics of Semiconductors, Paris, 1964* (Dunod Cie., Paris, 1964), p. 3.

[10] D. Brust, Phys. Rev. 134, A1337 (1964). J. C. Phillips, Phys. Rev. 112, 685 (1958).

By using $V_p(3)=-0.23$, $V_p(8)=0$, and $V_p(11)=0.06$ Ry for germanium and $V_p(3)=-0.21$, $V_p(8)=0.04$, and $V_p(11)=0.08$ Ry for silicon the eigenvalues listed in Table I were obtained. Also listed in Table I are the eigenvalues obtained by the O.P.W. method[9] and the eigenvalues used in the $\mathbf{k}\cdot\mathbf{p}$ Hamiltonian.

For the $\mathbf{k}\cdot\mathbf{p}$ Hamiltonian of germanium the experimental values of $E(\Gamma_{2'}{}^l)$ and $E(\Gamma_{15})$ have been corrected for the effects of the spin-orbit interaction (this interaction is present in the experimental data and its effect on the band structure will be treated later). For $E(\Gamma_1{}^l)$, $E(\Gamma_1{}^u)$, $E(\Gamma_{12'})$, and $E(\Gamma_{25'}{}^u)$, the O.P.W. values have been used while the $\Gamma_{2'}{}^u$ state has, somewhat arbitrarily, been taken slightly higher than the $\Gamma_{25'}{}^u$ state. The only justification for this is that $E(\Gamma_{2'}{}^u)$ lies somewhat higher than $E(\Gamma_{25'}{}^u)$ in the pseudopotential calculation (see Table I). The $\Gamma_{25'}{}^u$ and $\Gamma_{2'}{}^u$ states are coupled to the bands of interest by matrix elements (P' and P'') which are relatively small (see Table II), and hence small errors in the energies of these states will not affect the shape of the bands of interest. As will be discussed in more detail in the next section the band structure of germanium calculated by the $\mathbf{k}\cdot\mathbf{p}$ method using the O.P.W. eigenvalues at $\mathbf{k}=0$ is in better agreement with certain experimental data than is the band structure calculated using the pseudopotential eigenvalues.

For silicon, the experimental value of $E(\Gamma_{15})$ and the value of $E(\Gamma_{2'}{}^l)$ estimated from Ge-Si alloys are used in the $\mathbf{k}\cdot\mathbf{p}$ Hamiltonian. Since for silicon the $\Gamma_{25'}{}^u$ and $\Gamma_{2'}{}^u$ eigenvalues obtained from O.P.W. calculations are not available in the literature these eigenvalues, as well as the energies of the $\Gamma_1{}^u$ and $\Gamma_1{}^l$ states, were calculated by the pseudopotential method using Eqs. (11), (12), and (13). For $E(\Gamma_{12'})$ the free-electron energy $4(2\pi/a)^2$ was used. As opposed to germanium the calculated band structure of silicon using the pseudopotential eigenvalues at $\mathbf{k}=0$ gives excellent agreement with available experimental data. Also the eigenvalues at $\mathbf{k}=0$ obtained by O.P.W. calculations are quite close to the pseudopotential values.

The matrix elements of $\mathbf{p}$ obtained by the pseudopotential method for germanium and silicon are listed in Table II. Two of these matrix elements, P and Q, are accurately known from cyclotron-resonance experiments[11,12] and the values of the $E(\Gamma_{2'}{}^l)$ and $E(\Gamma_{15})$ energies. The matrix element R can be estimated from the value of $G=R^2/E(\Gamma_{12'})$ obtained from cyclotron resonance[11,12] and the calculated $E(\Gamma_{12'})$ energy. The values of P and Q are taken from the experimental data while the other eight matrix elements have been adjusted to fit the following experimental data: the energies of the L_1 conduction band and the $L_{3'}$ and L_3 states, the X_4-X_1 gap, the energy of the Δ_1 conduction-band minimum, and the position in $\mathbf{k}$ space of this minimum.[13] The matrix element P'' has only a very small effect on the bands of interest and hence is taken to have the pseudopotential value. The X_1 conduction-band degeneracy, required by symmetry, imposes another condition on the matrix elements of $\mathbf{p}$ and thus all the necessary matrix elements can be determined. When this procedure is followed, the X_1 valence-band degeneracy is not obtained due to the inaccuracies in $E(\Gamma_1{}^l)$. If this eigenvalue is shifted by an amount equal to the lower X_1 splitting and T' changed slightly so that $(T')^2/[E(\Gamma_1{}^l)-E(\Gamma_{15})]$ is kept constant, the required degeneracy is imposed and the remaining bands are not altered by any significant amount. The L_1 conduction band of silicon and the Δ_1 conduction-band energy of germanium are obtained by extrapolation from Ge-Si alloy data.[14] The $L_{3'}$ valence-band maximum is believed to be at about -1.2 eV for both germanium and silicon.[15] The position in $\mathbf{k}$ space of the lowest conduction-band minimum of silicon is known from ENDOR[16] measurements and we assume this minimum to be the same fraction of $2\pi/a$ away from $\mathbf{k}=0$ for germanium as for silicon.[13]

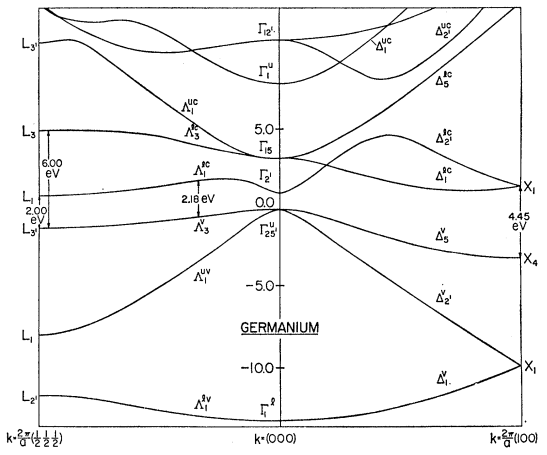

FIG. 2. Energy bands of germanium calculated by the $\mathbf{k}\cdot\mathbf{p}$ method in the [111] and [100] directions of $\mathbf{k}$ space.

The adjustment of the matrix elements of $\mathbf{p}$ so as to fit all the data given above is greatly aided by the factorization of the secular equation. The position in $\mathbf{k}$ space and the energy of Δ_1 conduction-band minimum determines T and T' uniquely [see Eq. (7)] and hence the energy of the X_1 conduction band. Since the X_4-X_1 gap is known from optical measurements,[8] the position

[11] B. W. Levinger and D. R. Frankl, J. Phys. Chem. Solids **20**, 281 (1961).

[12] J. C. Hensel and G. Feher, Phys. Rev. **129**, 1041 (1963).

[13] Recent measurement on diamond [J. L. Yarnell and J. L. Warren, Bull. Am. Phys. Soc. **10**, 385 (1965)] indicate that the distance from the zone center of the Δ_1 conduction-band minima is about the same for this material as for silicon, thus indicating that the position of this minima does not vary greatly for the group IV materials.

[14] R. Brauenstein, F. Herman, and A. R. Moore, Phys. Rev. **109**, 695 (1958); J. Tauc and A. Abraham, J. Phys. Chem. Solids **20**, 190 (1961).

[15] C. Hilsum, in *Proceedings of the International Conference on the Physics of Semiconductors, Paris, 1964* (Dunod Cie., Paris, 1964), p. 1127.

[16] G. Feher, Phys. Rev. **114**, 1219 (1959).

of X_4 is then determined and can be used to obtain Q' if Q is known [see Eq. (6)]. Similarly, once Q and Q' are known, it is possible to obtain R and R' from $E(L_3)$ and $E(L_{3'})$ by using Eq. (9). The determination of P' and P''' (if P is known) is somewhat more laborious due to the larger dimensionality of Eqs. (8) and (10), which must be solved simultaneously. P' and P''' are then varied until $E(L_1)$ agrees with the experimental value and the energy of the $\Delta_{2'}$ conduction band at the zone edge agrees with the value of $E(X_1)$ determined previously. This determination is greatly simplified by use of the projections of the states at L and X on the $\mathbf{k}=0$ states. The projections are obtained as eigenvector components in our computer program. The procedure used is the following: For the unknown matrix elements of $\mathbf{p}$, the pseudopotential values (or any other approximate values) are taken. Using these values the secular equation at X and L is solved and eigenvalues at L_1 and X_1 will, in general, differ somewhat from the known values. It is then possible to vary P' and P''' by a small amount, dP' and dP''', and calculate the corresponding variation of $E(L_1)$ and $E(X_1)$ from first-order perturbation theory. Making this variation equal to the amount required to obtain the desired values of $E(L_1)$ and $E(X_1)$ determines dP' and dP''' from which the correct values of P' and P''' can be obtained. It may be required to repeat this process several times in order to achieve convergence. The values of the matrix elements of $\mathbf{p}$ calculated by the above technique for germanium and silicon are listed in Table II.

V. ENERGY BANDS OF GERMANIUM AND SILICON

Figures 2 and 3 show the energy bands of germanium and silicon in the [100] and [111] direction. These bands were obtained by diagonalizing either the full 15×15 $\mathbf{k}\cdot\mathbf{p}$ Hamiltonian or the appropriate factorized matrices using an IBM-7070 computer. All the bands shown in Figs. 2 and 3, with the exception of the X_3 conduction band, reach the edge of the B.Z. with zero

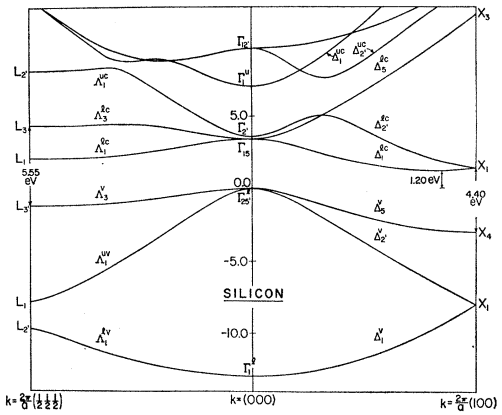

FIG. 3. Energy bands of silicon calculated by the $\mathbf{k}\cdot\mathbf{p}$ method in the [111] and [100] directions of $\mathbf{k}$ space.

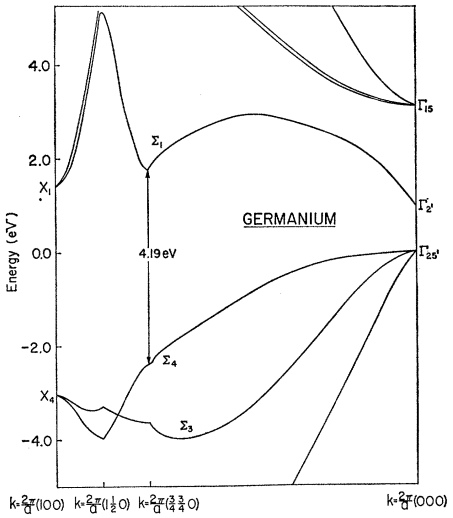

FIG. 4. Energy bands of germanium along the $X-W$, $W-K$, and $K-\Gamma$ lines as calculated by the $\mathbf{k}\cdot\mathbf{p}$ method.

slope or zero average slope (X_1 states) as required by crystal symmetry. The X_3 band is quite high in energy and its violation of this symmetry requirement is due either to our not having considered higher $\Gamma_{25'}$ states in the $\mathbf{k}\cdot\mathbf{p}$ Hamiltonian or to having taken too high an energy for $E(\Gamma_{25'}{}^u)$. Since no experimental effects of the X_3 band have been observed, no attempt will be made to bring its slope to zero at the edge of the zone.

The saddle point in the valence-conduction band separation ($\Lambda_3-\Lambda_1$), which is observed as a peak in the reflection spectrum of germanium at 2.29 eV, appears in Fig. 2 at 2.18 eV. This value compares favorably with the value obtained by Brust.[10] This saddle point is absent in silicon. In Figs. 2 and 3 there is another point inside the B.Z. for which $\nabla_{\mathbf{k}}(E_c-E_v)=0$ (E_c and E_v are the energies of a conduction and a valence band, respectively) in the [100] direction. The bands in-

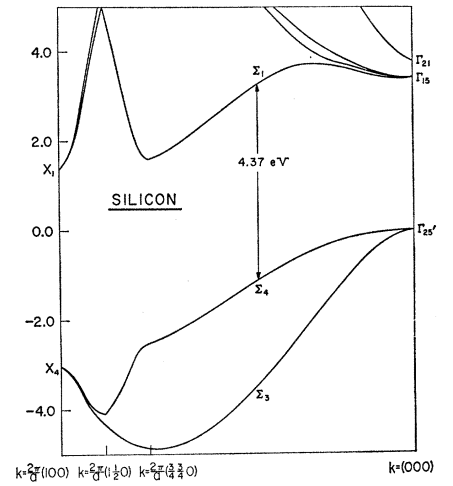

FIG. 5. Energy bands of silicon along the $X-W$, $W-K$, and $K-\Gamma$ lines as calculated by the $\mathbf{k}\cdot\mathbf{p}$ method.

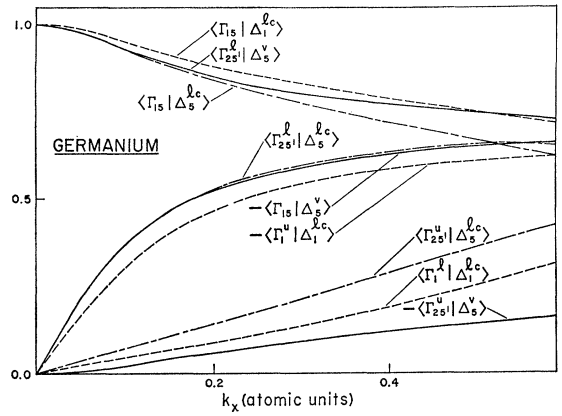

FIG. 6. Eigenvectors of the two lowest Δ_5 bands ($\Delta_5{}^v$,$\Delta_5{}^{lc}$) and the Δ_1 conduction band ($\Delta_1{}^{lc}$) as a function of k_x in germanium.

volved are the $\Delta_{2'}$ (conduction) and Δ_5 (valence). The values of E_c-E_v at these points are 6.4 eV for germanium and 6.3 eV for silicon. The matrix elements of $\mathbf{p}$ for these $\Delta_5-\Delta_{2'}$ transitions are somewhat smaller than for the $\Delta_3-\Delta_1$ transitions (see next section), but large enough for these transitions to be observable. These transitions should occur very near the $L_{3'}-L_3$ transitions and are probably responsible for the broad nature of the $L_{3'}-L_3$ reflection peak in silicon.[17] Similar transitions are likely to be responsible for the anomalies in the $L_{3'}-L_3$ spin-orbit splitting observed

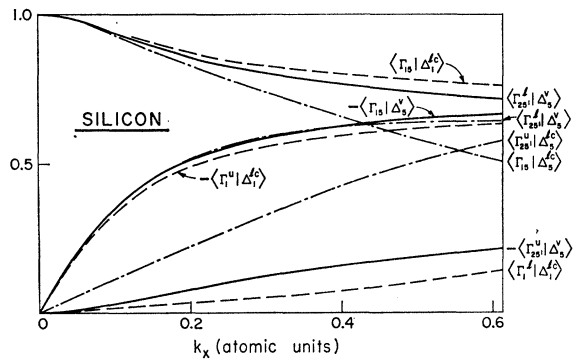

FIG. 7. Eigenvectors of the two lowest Δ_5 bands ($\Delta_5{}^v$,$\Delta_5{}^{lc}$) and the Δ_1 conduction band ($\Delta_1{}^{lc}$) as a function of k_x in silicon.

for many zinc-blende-type materials[18]: $\Delta_5-\Delta_{2'}$ transitions are seen superimposed on the $L_{3'}-L_3$ transitions.

Figures 4 and 5 show the calculated energy bands of germanium and silicon along the diagonal of the square face of the B.Z. ($X-W$, where the coordinates of the W point are $(2\pi/a)[1,\frac{1}{2},0]$), along the zone edge common to two hexagonal faces $\{W-K$, where $K=(2\pi/a)\times[\frac{3}{4},\frac{3}{4},0]\}$, and along the [110] direction (Σ). The $\Sigma_4-\Sigma_1$ singularity in the combined density of states (which together with the X_4-X_1 singularity is responsible for the main reflection peak) is calculated to have an energy difference of 4.2 eV in germanium (see Fig. 4) and 4.4 eV in silicon (see Fig. 5). These values are in good agreement with experimental data. When the band structure of Ge is calculated by the $\mathbf{k}\cdot\mathbf{p}$ method using the values of $E(\Gamma_1{}^l)$, $E(\Gamma_1{}^u)$, $E(\Gamma_{12'})$, $E(\Gamma_{25'}{}^u)$, and $E(\Gamma_{2'}{}^u)$ obtained by the pseudopotential technique [see Eqs. (11), (12), and (13)] the $\Sigma_4-\Sigma_1$

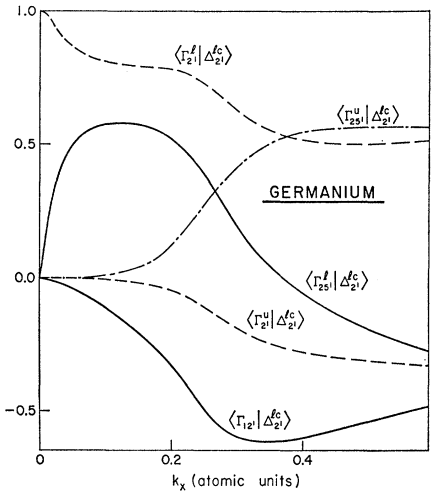

FIG. 8. Eigenvector components of the $\Delta_{2'}{}^{lc}$ state as a function of k_x in germanium.

gap has an energy of 3.5 eV. There is also a $\Sigma_3-\Sigma_1$ singularity, which has an energy difference of 6.5 eV for germanium and 6.9 eV for silicon. However, the matrix element associated with these optical transitions is very small (these matrix elements have been calculated from the eigenvectors which are reported later) and they are not likely to be observed.

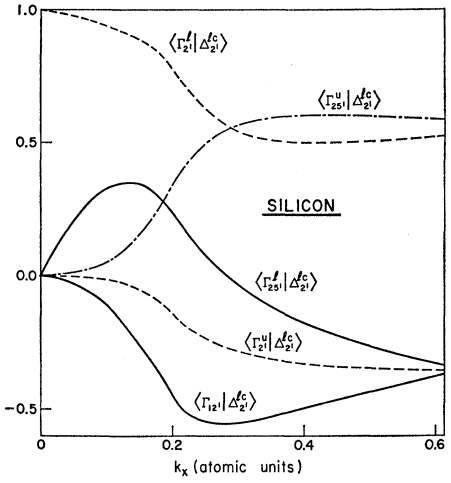

FIG. 9. Eigenvector components of the $\Delta_{2'}{}^{lc}$ state as a function of k_x in silicon.

[17] H. R. Philipp and H. Ehrenreich, Phys. Rev. 125, 1550 (1963).
[18] M. Cardona, in *Proceedings of the International Conference on the Physics of Semiconductors, Paris, 1964* (Dunod Cie., Paris, 1964), p. 181.

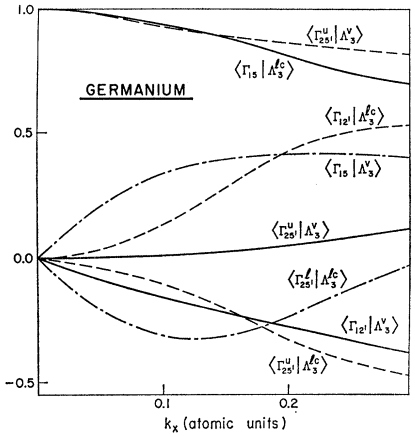

FIG. 10. Eigenvector components of the Λ_3^v and the Λ_3^{lc} states in germanium as a function of k_x.

The components of the eigenvectors obtained from the computer program are the coefficients of the expansion of the periodic part of the Bloch function in terms of the 15 Bloch functions at $\mathbf{k}=0$ which have been taken as basis states. The variation of these coefficients with $\mathbf{k}$ for the states of most interest along [100] and [111] will be given. Figures 6 and 7 show the eigenvectors of the two lowest Δ_5 bands ([100] direction), labeled Δ_5^v (valence band) and Δ_5^{lc} (lower conduction band), and the lower Δ_1 conduction band (Δ_1^{lc}) as obtained from Eqs. (6) and (7). The components of the eigenvector of the lower $\Delta_{2'}$ conduction band ($\Delta_{2'}^{lc}$) are obtained from Eq. (8) and are shown in Fig. 8 for germanium and Fig. 9 for silicon.

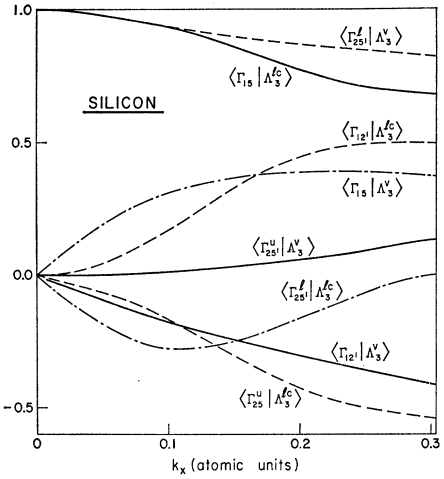

FIG. 11. Eigenvector components of the Λ_3^v and the Λ_3^{lc} states in silicon as a function of k_x.

The eigenvectors of the Λ_3^v and the Λ_3^{lc} band are obtained from Eq. (9) and are shown in Fig. 10 for germanium and in Fig. 11 for silicon.

The eigenvectors of the lowest conduction band Λ_1^{lc} in the [111] direction as obtained from Eq. (10) are shown in Fig. 12 for germanium and Fig. 13 for silicon.

The knowledge of the eigenvectors in terms of the basis at $\mathbf{k}=0$ enables one to calculate matrix elements of physical quantities at any point in $\mathbf{k}$ space in terms of the matrix elements at $\mathbf{k}=0$. As an example, it is possible to calculate the matrix elements of the linear momentum $\mathbf{p}$ which are needed for the determination of the optical transition probabilities or effective masses.

Figure 14 shows the matrix elements of p_y between the upper valence band in the [100] direction (Δ_5^v) and the two lower conduction bands (Δ_1^{lc},$\Delta_{2'}^{lc}$). These matrix elements determine most of the ultraviolet behavior of these materials. As shown in Fig. 14 $\langle\Delta_{2'}^{lc}|p_y|\Delta_5^v\rangle$, at the point where the density of states singularity occurs, is somewhat stronger in silicon than in germanium. This may be the reason why the shoulder of the $\Lambda_{3'}-\Lambda_3$ reflection peak, which we have earlier attributed to this $\Delta_5-\Delta_{2'}$ singularity, is stronger in silicon than in germanium.

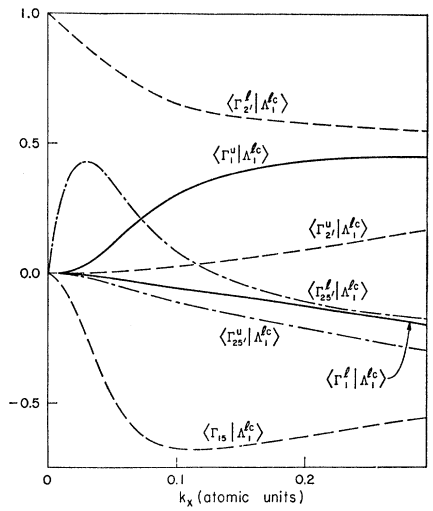

FIG. 12. Components of the Λ_1^{lc} eigenstate as a function of k_x in germanium.

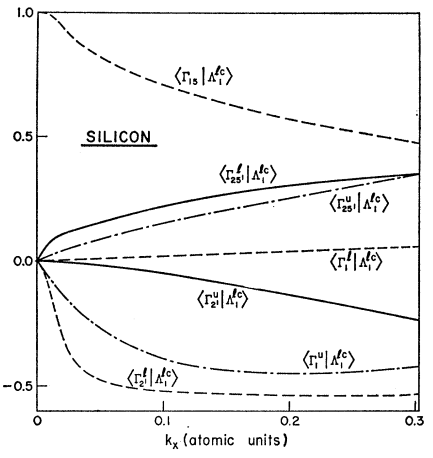

FIG. 13. Components of the Λ_1^{lc} eigenstate as a function of k_x in silicon.

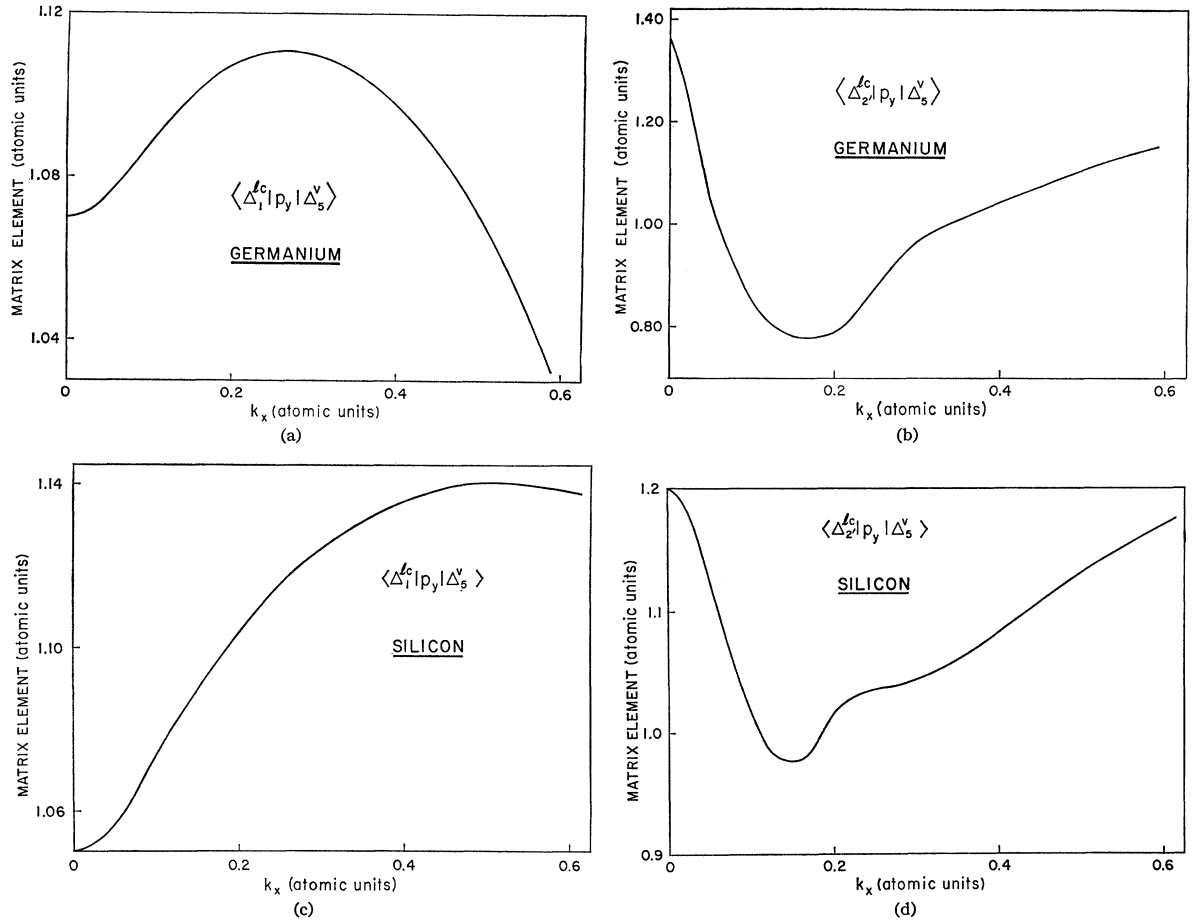

FIG. 14. Matrix elements of p_y between $\Delta_1{}^{lc}$ and $\Delta_5{}^v$ and between $\Delta_{2'}{}^{lc}$ and $\Delta_5{}^v$ as a function of k_x in germanium and silicon.

Figure 15 shows the matrix elements of $\bar{p}_z$ ($\bar{p}_z$ is the component of $\mathbf{p}$ in the [111] direction) and of $\bar{p}_x$ ($\bar{p}_x$ is the component of $\mathbf{p}$ perpendicular to [111]) between the $\Lambda_3{}^v$ and $\Lambda_3{}^{lc}$ states for germanium and silicon. These matrix elements determine the transition probability for the $L_{3'}{}^v - L_3$ transitions seen in the reflectivity spectrum. As seen from Fig. 15, the $\bar{p}_z$ matrix element is much smaller than that of $\bar{p}_x$ and the optical transitions should occur at each set of valleys mainly for $\mathbf{p}$ perpendicular to the valley orientation. While these polarization effects are not observable for cubic material they will be important in interpreting the effect of uniaxial stress on the reflection spectrum.

Figure 16 shows the matrix elements of $\bar{p}_x$ between $\Lambda_3{}^v$ and $\Lambda_1{}^{lc}$. This matrix element varies only slightly through the B.Z. and is quite large. It determines the transition probability for the $\Lambda_3 - \Lambda_1$ transition in germanium. Also shown in Fig. 16 is the matrix element of $\bar{p}_z$ between $\Lambda_1{}^{lc}$ and $\Lambda_1{}^{uv}$. This matrix element is quite small, except in the neighborhood of $\mathbf{k}=0$, and hence the corresponding transitions are not to be seen in the optical spectra. Actually this matrix element must be exactly zero at the edge of the B.Z. (L) because of parity. The extremely small value of this matrix element at L (see Fig. 16) is an indication of the accuracy of the $\mathbf{k}\cdot\mathbf{p}$ expansion. It has been observed from Figs. 14, 15, and 16 and other calculated matrix elements of $\mathbf{p}$ that whenever transitions between two bands are forbidden by symmetry at either the center or the edge of the B.Z., they remain quite improbable inside the zone even if they are allowed by symmetry. This could be quite useful in the selection of the transitions which are likely to cause structure in the optical properties. This observation and the small value of the T' matrix element explains why no transitions involving the lowest valence band are seen for these materials.

The effective masses obtained from our eigenvectors and energy gaps by the $\mathbf{k}\cdot\mathbf{p}$ technique at the $L_1{}^{lc}$ point, the $\Delta_1{}^{lc}$ minimum, and the $\Gamma_{2'}{}^l$ point are listed in Table III together with the available experimental values. Also listed in Table III are the band parameters A, B, and C at $\Gamma_{25'}{}^l$, and their experimental values. Listed in Table IV are the calculated masses at $\Gamma_1{}^u$ and $\Gamma_1{}^l$, the calculated band parameters a, b, and c for the Γ_{15} band (analogous to the A, B, and C's of $\Gamma_{25'}$), and the parameter K which determines the expansion

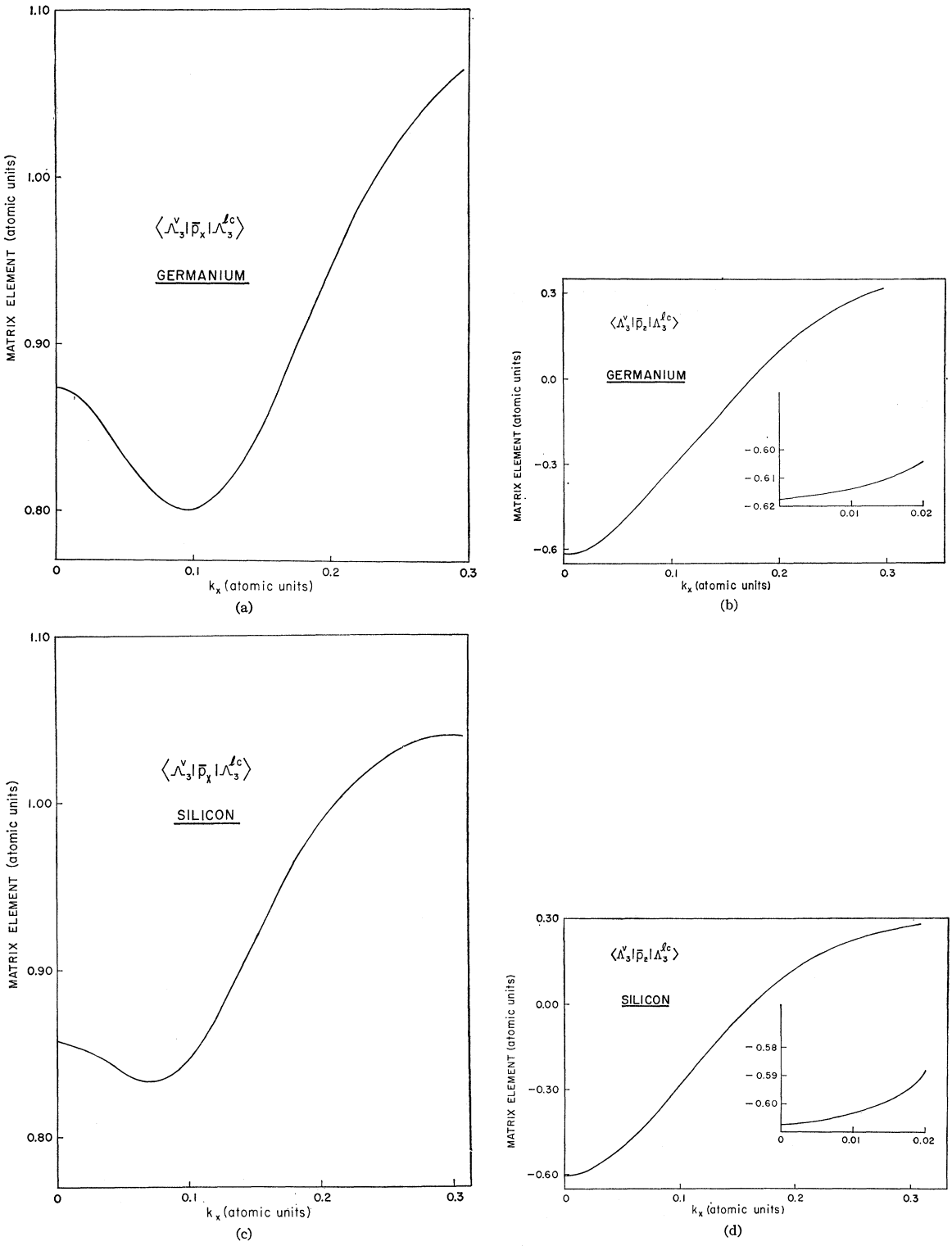

FIG. 15. Matrix elements of $\bar{p}_x$ and $\bar{p}_z$ between Λ_3^v and Λ_3^{lc} as a function of k_x for germanium and silicon.

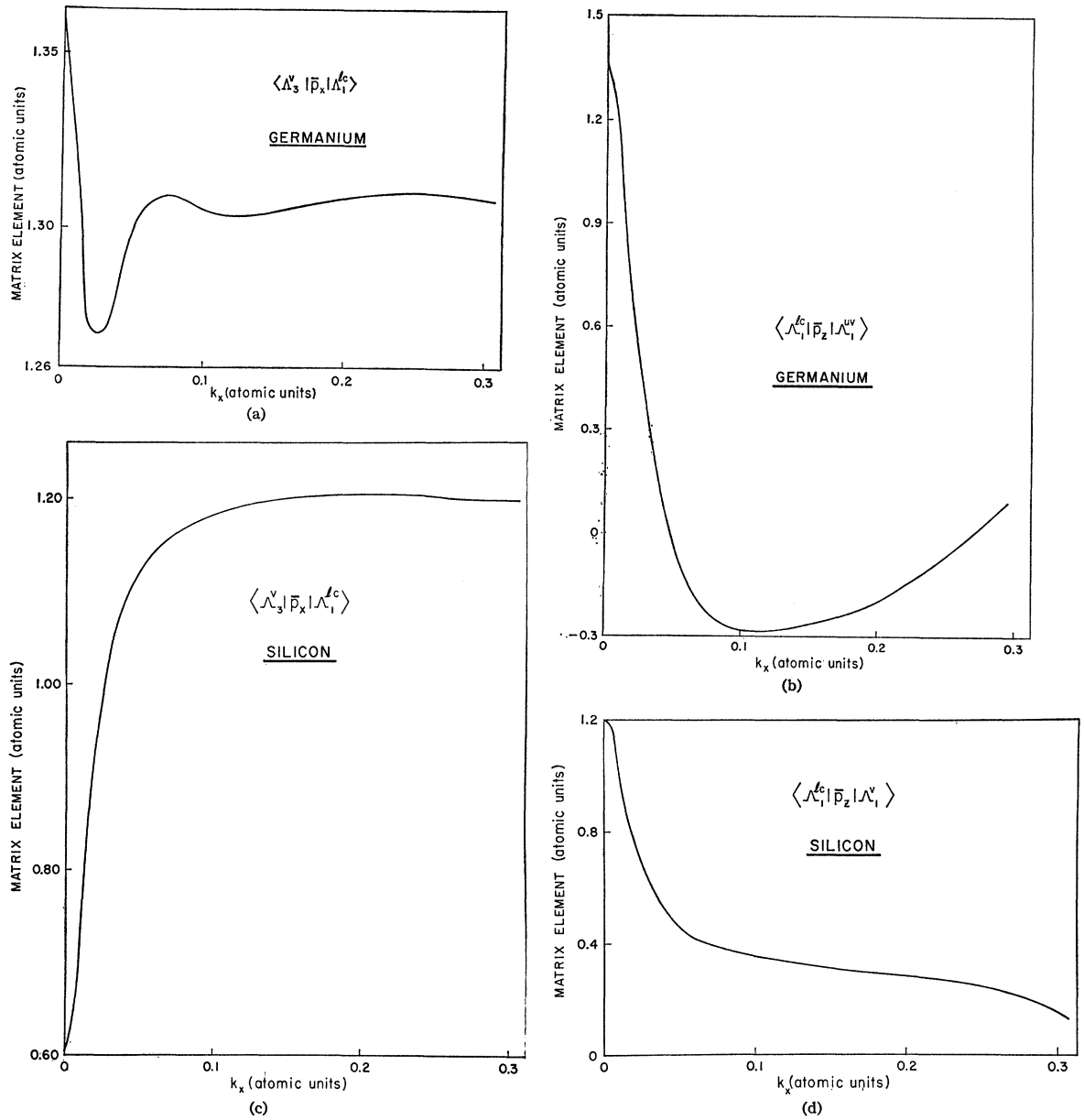

FIG. 16. Matrix elements of $\bar{p}_x$ between Λ_3^v and Λ_1^{lc} and matrix elements of $\bar{p}_z$ between Λ_1^{lc} and Λ_1^{uv} for germanium and silicon.

of the $\Gamma_{12'}$ band around $\mathbf{k}=0$:

$$(K+1)k^2+K[k^4-3(k_x^2k_y^2+k_y^2k_z^2+k_z^2k_x^2)]^{1/2},$$

where

$$K=\frac{R^2}{E(\Gamma_{12'})}-\frac{(R')^2}{E(\Gamma_{25'}{}^u)-E(\Gamma_{12'})}.$$

VI. SPIN-ORBIT COUPLING FOR GERMANIUM

The inclusion of the $\mathbf{k}$-independent spin-orbit interaction Hamiltonian of Eq. (4) in the $\mathbf{k}\cdot\mathbf{p}$ Hamiltonian does not present, in principle, any serious difficulty. The spin degeneracy doubles the dimensionality of the matrix. The 30×30 matrix so obtained has some imaginary matrix elements. Our computer subroutine requires an additional doubling of the matrix dimension when complex matrices are to be diagonalized. Hence the completed diagonalization of the $\mathbf{k}\cdot\mathbf{p}$ plus spin-orbit Hamiltonian requires the diagonalization of a 60×60 real matrix. Speed and storage limitations in our computer prevented us from handling the problem this way. The problem can be considerably simplified by making some approximations.

Consider how many new parameters are required for treating the spin-orbit interaction. The spin-orbit Hamiltonian couples the states of $\Gamma_{25'}$ symmetry with states of $\Gamma_{25'}$, Γ_1, and $\Gamma_{12'}$ symmetry. It also couples the Γ_{15} states with itself and with $\Gamma_{2'}$ states. The $\Gamma_{25'}{}^l$ state

TABLE III. Calculated and experimental values of the band parameters at L_1^{lc}, the Δ_1^{lc} minimum, $\Gamma_{2'}{}^l$, and $\Gamma_{25'}{}^l$ for germanium and silicon. The effective masses are given in units of the free-electron mass.

		Germanium	Silicon
$m_{\parallel}^*(L_1^{lc})$	calc.	1.349	1.418
	exptl.	1.588[a]	
$m_{\perp}^*(L_1^{lc})$	calc.	0.0791	0.130
	exptl.	0.0815[a]	
$m_{\parallel}^*(\Delta_1^{lc})$	calc.	0.7991	0.9716
	exptl.		0.9163[b]
$m_{\perp}^*(\Delta_1^{lc})$	calc.	0.200	0.1945
	exptl.		0.1905[b]
$m^*(\Gamma_{2'}{}^l)$	calc.	0.038	0.156
	exptl.	0.041[c]	
A	calc.	−12.35	−4.38
	exptl.	−13.27[a]	−4.28[d]
B	calc.	−8.26	−1.00
	exptl.	−8.63[a]	−0.75[d]
$\|C\|$	calc.	12.07	4.80
	exptl.	12.4[a]	5.25[d]

[a] Reference 11.
[b] J. C. Hensel, H. Hasegawa, and M. Nakayama, Phys. Rev. **138**, A225 (1965).
[c] Reference 3.
[d] J. C. Hensel and G. Feher, Phys. Rev. **129**, 1041 (1963).

behaves like a p state near the atomic core. Hence the matrix elements $\langle\Gamma_{25'}{}^l|H_{so}|\Gamma_1{}^u\rangle$, $\langle\Gamma_{25'}{}^l|H_{so}|\Gamma_1{}^l\rangle$, $\langle\Gamma_{25'}{}^l|H_{so}|\Gamma_{25'}{}^u\rangle$, and $\langle\Gamma_{25'}{}^l|H_{so}|\Gamma_{12'}\rangle$ are quite small because of the predominantly s- and d-like nature of the states on the right-hand side. They are assumed to be equal to zero. Similarly, the matrix elements $\langle\Gamma_{15}|H_{so}|\Gamma_{2'}{}^u\rangle$ and $\langle\Gamma_{15}|H_{so}|\Gamma_{2'}{}^l\rangle$ are assumed to be equal to zero. The spin-orbit Hamiltonian is then determined by the following three matrix elements:

$$\Delta_{so}(\Gamma_{15})=3i(\alpha/2)^2\langle x(\Gamma_{15})|(\nabla V\times\mathbf{p})_z|y(\Gamma_{15})\rangle,$$
$$\Delta_{so}(\Gamma_{25'}{}^l)=3i(\alpha/2)^2\langle X(\Gamma_{25'}{}^l)|(\nabla V\times\hat{p})_z|Y(\Gamma_{25'}{}^l)\rangle, \quad (14)$$
$$\Delta_{so}(\Gamma_{25'}{}^u)=3i(\alpha/2)^2\langle X(\Gamma_{25'}{}^u)|(\nabla V\times\hat{p})_z|Y(\Gamma_{25'}{}^u)\rangle.$$

These parameters are close to the corresponding parameters for atomic germanium. Hence it is assumed that $\Delta_{so}(\Gamma_{25'}{}^u)\approx 0$ since the spin-orbit splitting of the $4d$ levels of atomic germanium is only 5% of the $4p$ splitting. For germanium $\Delta_{so}(\Gamma_{25'}{}^l)$ is known experimentally to be 0.29 eV. The Λ_3 spin-orbit splitting at $k_x=0.1$ observed experimentally[19] (0.195 eV) makes it possible to determine the spin-orbit coupling parameter $\Delta_{so}(\Gamma_{15})$. For this value of $\mathbf{k}$, the spin-orbit splitting of Λ_3 can be treated as being produced by the first-order term in H_{so}. By using the wave-function expansion of Fig. 10 it is found that $\Delta_{so}(\Gamma_{15})=0.36$ eV. In order to check this procedure the spin-orbit splitting at X_4 has been calculated from the above values of $\Delta_{so}(\Gamma_{25'}{}^l)$ and $\Delta_{so}(\Gamma_{15})$. It is found to be almost ex-

TABLE IV. Calculated values of the band parameters at $\Gamma_1{}^u$, $\Gamma_1{}^l$, Γ_{15}, and $\Gamma_{12'}$ for germanium and silicon. The effective masses are given in units of the free-electron mass.

	Germanium	Silicon
$m^*(\Gamma_1{}^u)$	0.1905	0.1868
$m^*(\Gamma_1{}^l)$	1.310	1.037
a	2.686	1.847
b	−2.850	−2.582
$\|c\|$	4.926	4.442
K	−3.453	−5.395

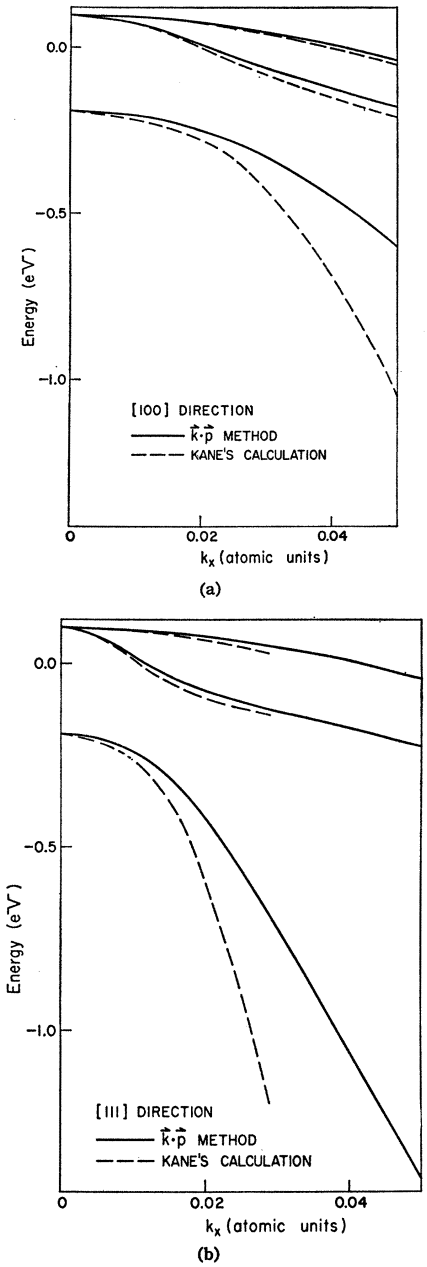

FIG. 17. Upper valence bands in germanium along the [100] and [111] directions including spin-orbit interaction. The early calculations of Kane [E. O. Kane, J. Chem. Phys. Solids **1**, 82 (1956)] are also shown.

[19] F. Lukes and E. Schmidt, in *Proceedings of the International Conference on the Physics of Semiconductors, Exeter, 1962* (Institute of Physics and the Physical Society, London, 1962), p. 389.

actly zero (0.0023 eV) as required by symmetry. By this technique it is now quite easy to calculate the spin-orbit splitting at Λ_3^{1c}, Λ_3^{v}, Δ_5^{v}, and Δ_5^{1c} for $k_x>0.05$. For smaller values of k_x the Λ_1^{uv} and $\Delta_{2'}{}^{v}$ states must also be taken into account. We have diagonalized a spin-orbit Hamiltonian which includes the three upper valence bands and the lowest conduction band for $k_x<0.05$. The matrix elements were obtained from $\Delta_{so}(\Gamma_{25'}{}^{l})$, $\Delta_{so}(\Gamma_{15})$, and the eigenvectors of Figs. 6, 8, 10, and 12. The results are presented in Fig. 17 together with the early calculations of Kane.[3] The large discrepancy between our results and Kane's for the split-off band is due to our more accurate treatment and to our smaller value of G which seems to agree better with recent data.[11] The spin-orbit splitting of Λ_3^{v}, Λ_3^{1c}, and Δ_5^{v} calculated by first-order perturbation theory is given in Fig. 18. This splitting is accurate for $k_x>0.05$.

VII. PRESSURE DEPENDENCE OF THE BAND STRUCTURE OF GERMANIUM

The $\mathbf{k}\cdot\mathbf{p}$ expansion of the Bloch functions $u_{n,\mathbf{k}}(\mathbf{r})$ in terms of $u_{n,0}(\mathbf{r})$ makes it possible to calculate the pressure dependence of the energy bands in terms of the pressure dependence of the states at $\mathbf{k}=0$. Unfortunately only the pressure coefficients of the $\Gamma_{25'}{}^{l}-\Gamma_{2'}{}^{l}$ gap of germanium[20] and the $\Gamma_{25'}{}^{l}-\Gamma_{15}$ gap of silicon[21] are known experimentally. However, it is possible to use the pseudopotential scheme discussed in Sec. V for the calculations of the pressure coefficients of the various states at $\mathbf{k}=0$.[22] These coefficients are obtained as linear combinations of the pressure coefficients of the three pseudopotential components $V(3)$, $V(8)$, and $V(11)$ plus the effect of the change in lattice constant. Bassani and Brust[22] have attempted to calculate $dV(3)/dP$, $dV(8)/dP$, and $dV(11)/dP$ by using approximate expressions for the crystal potential and the orthogonalization terms. They showed that the contribution of $V(3)$ to the pressure effects is very small. We shall show that good agreement with all observed pressure coefficients is obtained if one assumes that only $V(11)$ changes with pressure and one treats this change as an adjustable parameter.

Under this assumption and treating the changes in $V(11)$ and in the lattice constant by first-order perturbation theory one obtains from the $\mathbf{k}=0$ wave functions of Sec. V:

$$
\begin{aligned}
&\frac{dE(\Gamma_1{}^{u})}{dP}=-1.840\frac{d(\ln a)}{dP},\quad \frac{dE(\Gamma_1{}^{l})}{dP}=-0.256\frac{d(\ln a)}{dP},\quad \left\langle\Gamma_1{}^{u}\left|\frac{dH}{dP}\right|\Gamma_1{}^{l}\right\rangle=-0.681\frac{d(\ln a)}{dP},\\
&\frac{dE(\Gamma_{2'}{}^{u})}{dP}=-2.579\frac{d(\ln a)}{dP}-3.191\frac{dV(11)}{dP},\quad \frac{dE(\Gamma_{2'}{}^{l})}{dP}=-2.310\frac{d(\ln a)}{dP}\\
&\qquad\qquad +3.191\frac{dV(11)}{dP},\quad \left\langle\Gamma_{2'}{}^{u}\left|\frac{dH}{dP}\right|\Gamma_{2'}{}^{l}\right\rangle=-0.322\frac{d(\ln a)}{dP}+1.316\frac{dV(11)}{dP},\\
&\frac{dE(\Gamma_{25'}{}^{u})}{dP}=-2.581\frac{d(\ln a)}{dP}+1.846\frac{dV(11)}{dP},\quad \frac{dE(\Gamma_{25'}{}^{l})}{dP}=-2.308\frac{d(\ln a)}{dP},\\
&\qquad\qquad -1.846\frac{dV(11)}{dP},\quad \left\langle\Gamma_{25'}{}^{u}\left|\frac{dH}{dP}\right|\Gamma_{25'}{}^{l}\right\rangle=-0.321\frac{d(\ln a)}{dP}-0.784\frac{dV(11)}{dP},\\
&\frac{dE(\Gamma_{15})}{dP}=-2.095\frac{d(\ln a)}{dP},\quad \frac{dE(\Gamma_{12'})}{dP}=-2.794\frac{d(\ln a)}{dP}.
\end{aligned}
\tag{15}
$$

From the known pressure dependence of the $\Gamma_{25'}{}^{l}-\Gamma_{2'}{}^{l}$ gap[20] and the compressibility of germanium[23] one obtains $dV(11)/dP=0.0019$ Ry/kbar. Using Eqs. (15) and the $\mathbf{k}\cdot\mathbf{p}$ wave functions as discussed in Sec. V, one obtains for the various gaps of germanium the pressure coefficients listed in Table V. In this table are also listed the experimental values of these pressure coefficients for germanium with the exception of the coefficients of the $\Gamma_{25'}{}^{l}-\Delta_1{}^{1c}$, the $\Gamma_{25'}{}^{l}-\Gamma_{15}$, and the X_4-X_1 gaps for which we have listed the values for silicon (values for germanium are not available).

It is generally accepted[24] that the pressure coefficients of the same gaps of germanium and silicon are very close. The agreement between the experimental and calculated values shown in Table V is excellent.

VIII. FURTHER APPLICATIONS OF THE k·p METHOD

The $\mathbf{k}\cdot\mathbf{p}$ technique is particularly suitable for calculating the band structure of zinc-blende-type compounds

[20] M. Cardona and W. Paul, J. Phys. Chem. Solids **17**, 138 (1960).
[21] W. Paul and D. M. Warshauer, J. Phys. Chem. Solids **5**, 102 (1958).
[22] F. Bassani and D. Brust, Phys. Rev. **131**, 1524 (1963).
[23] M. E. Fine, J. Appl. Phys. **26**, 862 (1955).
[24] R. Zallen and W. Paul, Phys. Rev. **134**, A1628 (1964).

TABLE V. Calculated and experimental values of the pressure coefficients of several energy gaps in germanium. The experimental values for the $\Gamma_{25'}{}^{l}-\Gamma_{15}$, X_4-X_1, and $\Gamma_{25'}{}^{l}-\Delta_1{}^{lc}$ gaps of silicon are given since the values for germanium are not available.

	Calculated (10^{-6} eV/atm)	Experimental (10^{-6} eV/atm)
$\Gamma_{25'}{}^{l}-\Gamma_{2'}{}^{l}$	13	13[a]
$\Gamma_{25'}{}^{l}-\Gamma_{15}$	3.5	5[b](Si)
$\Lambda_3{}^{v}-\Lambda_1{}^{lc}$	7	7.5[b]
X_4-X_1	2.3	3[b](Si)
$\Gamma_{25'}{}^{l}-L_1$	4.5	5[c]
$\Gamma_{25'}{}^{l}-\Delta_1{}^{lc}$	−1.6	−1.5[c](Si)

[a] Reference 20.
[b] R. Zallen, Gordon McKay Laboratory of Applied Science, Harvard University, Technical Report HP-12, 1964 (unpublished).
[c] Reference 21.

from the band structure of isoelectronic group IV materials.[25] The transition from a group IV to a zinc-blende material is accomplished by the application of a small antisymmetric potential which mixes states of opposite parity in the group IV material. This antisymmetric potential adds six independent matrix elements to the 15×15 $\mathbf{k}\cdot\mathbf{p}$ Hamiltonian. Hence, starting with the band parameters of the group IV isoelectronic material and varying the six matrix elements of the antisymmetric potential it should be possible to fit the experimental information available for the III–V and II–VI compounds. These calculations may settle a number of unresolved questions such as why for some zinc-blende materials the lowest energy reflection peak is caused by transitions at Λ while for others it is caused by Γ transitions. Preliminary calculations for GaAs indicate that the saddle point in the [110] direction ($\Sigma_4-\Sigma_1$) corresponds to an energy of 5.2 eV and produces the strong peak seen in the reflection spectrum at 5.1 eV.

It might also be possible to obtain the energy bands of wurtzite-type materials from the bands of the corresponding zince-blende compounds. In wurtzite the number of atoms per unit cell is double that of zinc-blende and hence the volume of the B.Z. is reduced by a factor of 2. This introduces extra states at $\mathbf{k}=0$ and hence a number of additional parameters in the $\mathbf{k}\cdot\mathbf{p}$ analysis.

As we have shown, this method is very well suited for energy-band calculations which include the spin-orbit interaction. Such calculations should be of interest in materials whose constituents have large atomic numbers such as gray tin, CdTe, InSb, etc.

The $\mathbf{k}\cdot\mathbf{p}$ technique is valuable for the calculation of band structures of materials in which large relativistic effects are present since some relativistic corrections are incorporated into the energy gaps and band parameters at $\mathbf{k}=0$, which are determined by fitting experimental data.

[25] M. Cardona and F. H. Pollak, Bull. Am. Phys. Soc. **10**, 615 (1965).

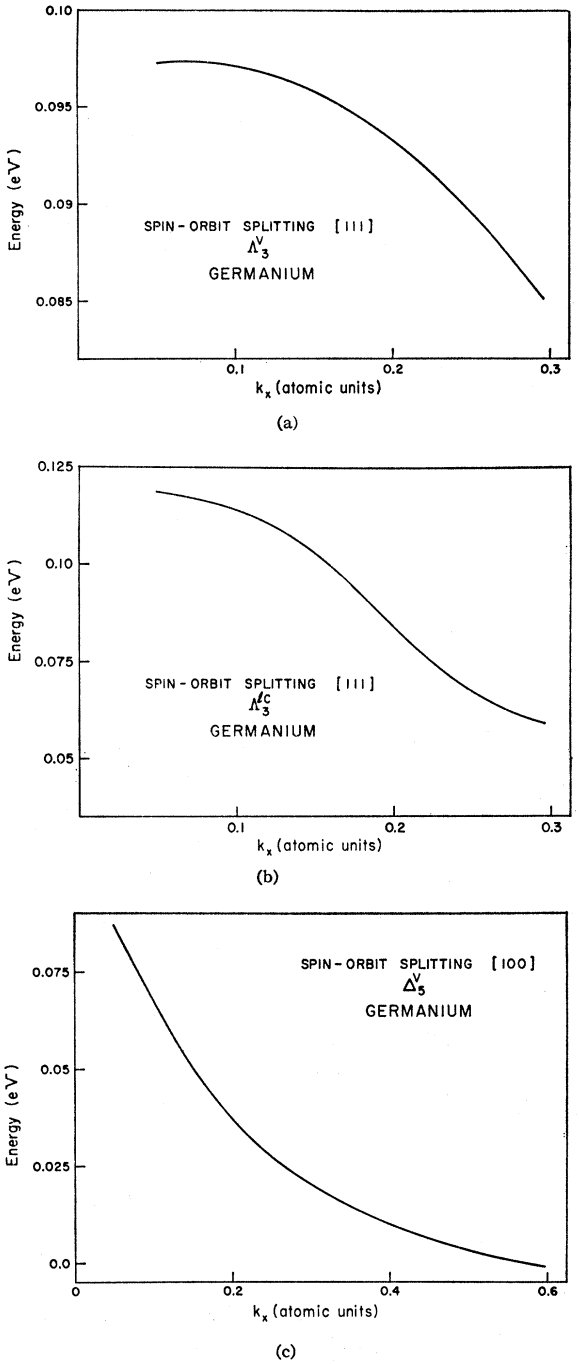

FIG. 18. First-order spin-orbit splittings of $\Lambda_3{}^{v}$, $\Lambda_3{}^{lc}$, and $\Delta_5{}^{v}$ for germanium accurate for $k_x>0.05$.